Tetranuclear manganese carboxylate clusters with imidazole-carboxylate chelating ligands. X-ray crystal structure of the 4-imidazoleacetate complex

Colette Boskovic, Kirsten Folting, George Christou *

Department of Chemistry and Molecular Structure Center, Indiana University, Bloomington, IN 47405-4001, USA

Abstract

Procedures are described for the synthesis of tetranuclear manganese carboxylate complexes with ligands derived from 4-imidazoleacetic acid (imidacH) and 4-imidazolecarboxylic acid (imidcarbH). Reaction mixtures containing NBu_4^nimidac or $NHex_4^n$imidcarb generated in situ and either $[Mn_3O(O_2CMe)_6(py)_3](ClO_4)$ or $Mn(O_2CR)_2$, RCO_2H (R = Me, Ph) and $NR_4'MnO_4$ (R' = Bu^n, Hex^n) give red–brown solutions from which the products $(NBu_4^n)[Mn_4O_2(O_2CR)_7(imidac)_2]$ (R = Me (**1**); R = Ph (**2**)) and $(NHex_4^n)[Mn_4O_2(O_2CR)_7(imidcarb)_2]$ (R = Me (**3**); R = Ph (**4**)) can be obtained. The X-ray crystal structure of **2** reveals that the anion consists of an $[Mn_4(\mu_3\text{-}O)_2]^{8+}$ core with the four Mn atoms disposed in a 'butterfly' arrangement and the O atoms triply bridging each 'wing'. Peripheral ligation is provided by seven bridging O_2CPh^- ligands and two chelating imidac$^-$ groups. All available characterization data are consistent with the same core for complexes **1**, **3** and **4**, with the structures varying only in the peripheral ligation. ^1H NMR spectroscopy of all four complexes indicates that the structure is maintained in solution and the majority of the resonances have been assigned on the basis of T_1 measurements and substitution and exchange experiments. Cyclic voltammetry reveals the presence of a single quasi-reversible oxidation processes for complexes **1** and **2**. © 2000 Elsevier Science Ltd. All rights reserved.

Keywords: Polynuclear manganese-carboxylate clusters; Imidazole-carboxylate chelating ligands; Paramagnetic NMR

1. Introduction

The chemistry of Mn carboxylate clusters is an area of considerable interest, and numerous examples varying widely in both nuclearity and structure have been reported [1]. The interest in these species is in part due to their application to the modeling of Mn-containing proteins and enzymes, in which up to four Mn nuclearities have been identified [2,3]. We have previously described procedures that allow the synthesis of tetranuclear Mn carboxylate compounds possessing the $[Mn_4(\mu_3\text{-}O)_2]$ core and of formulation $[Mn_4^{III}O_2(O_2CR)_7(L)_2]^z$, where L is a pyridine-based N/N or N/O chelate derived from 2,2'-bipyridine (bpy), picolinic acid (picH), 8-hydroxyquinoline (hqnH) or 2-(hydroxymethyl)pyridine (hmpH) [4–6].

As part of a continuing exploration of tetranuclear Mn carboxylate clusters with chelating ligands, we have recently turned our attention to the use of imidazole-containing chelates in order to compare and contrast the products with those already obtained with pyridine-based chelates. We describe herein our initial results comprising the syntheses and characterization of tetranuclear clusters possessing imidazole-based N/O chelating ligands derived from 4-imidazoleacetic acid (imidacH) and 4-imidazolecarboxylic acid (imidcarbH). These species allow informative comparisons with those possessing pyridine-based chelating ligands with which they are isostructural, as well as providing access to compounds that possess either five- or six-membered chelate rings but are otherwise identical. In addition, imidazole ligation to tetranuclear Mn clusters is of interest due to the histidine ligation of the tetranuclear Mn complex responsible for water oxidation in Photosystem II [7].

* Corresponding author. Tel.: + 1-812-855-2399; fax: + 1-812-855-2399.

imidacH   imidcarbH
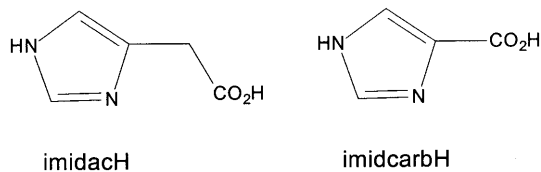
2. Experimental

2.1. Synthesis

All manipulations were performed under aerobic conditions, using materials as received. Trinuclear [Mn$_3$O] complexes were available from previous work [8]. NBu$_4^n$MnO$_4$ and Mn(O$_2$CPh)$_2$·2H$_2$O were prepared as described [4,9] and NHex$_4^n$OH (Hex = hexyl) was prepared according to Giovannellio et al. [10]. WARNING: Appropriate care should be taken in the use of NR$_4^n$MnO$_4$, and readers are referred to the detailed warning given elsewhere [9].

2.1.1. NHex$_4^n$MnO$_4$

To a vigorously stirred solution of KMnO$_4$ (5.00 g, 31.6 mmol) in H$_2$O (100 cm^3) was added a solution of NHex$_4^n$Br (13.50 g, 31.6 mmol) in H$_2$O (100 cm^3), resulting in the formation of a purple precipitate. This was filtered, washed copiously with H$_2$O and Et$_2$O and dried in vacuo at room temperature. The yield was 13.49 g, 92%.

2.1.2. (NBu$_4^n$)[Mn$_4$O$_2$(O$_2$CMe)$_7$(imidac)$_2$] (1)

Method A: to a stirred solution of Mn(O$_2$CMe)$_2$·4H$_2$O (0.74 g, 3.0 mmol) and glacial acetic acid (1 cm^3) in MeCN (70 cm^3) was slowly added NBu$_4^n$MnO$_4$ (0.27 g, 0.75 mmol) in small portions to give a deep brown solution. To this was added a solution resulting from the combination of imidacH·HCl (0.31 g, 1.9 mmol) in MeCN (5 cm^3) and 1.0 M NBu$_4^n$OH in MeOH (3.8 cm^3, 3.8 mmol). The reaction mixture was stirred overnight and a brown precipitate removed by filtration. The filtrate was reduced in volume to 50 cm^3 and Et$_2$O (100 cm^3) was added, leading to the formation of a red–brown precipitate which could be recrystallized from MeCN–Et$_2$O. The yield was 0.60 g (55%). Drying in vacuo leads to the unsolvated form. Elemental analysis, Anal. Found: C, 41.09; H, 5.78; N, 6.08. Calc. for C$_{40}$H$_{67}$N$_5$O$_{20}$Mn$_4$: C, 41.50; H, 5.83; N, 6.05. Selected IR data (cm^{-1}): 1647(m), 1608(s), 1493(m), 1467(w), 1401(s), 1387(s), 1333(s), 1320(s), 1266(w), 1227(w), 1176(w), 1087(w), 1028(m), 943(m), 935(sh), 882(w), 802(w), 737(sh), 721(m), 678(m), 650(s), 635(sh), 613(m), 436(m).

Method B: to a stirred solution of [Mn$_3$O(O$_2$CMe)$_6$(py)$_3$](ClO$_4$) (0.30 g, 0.34 mmol) in MeCN (20 cm^3) was added a solution resulting from the combination of imidacH·HCl (0.11 g, 0.68 mmol) in MeCN (3 cm^3) and 1.0 M NBu$_4^n$OH in MeOH (1.4 cm^3, 1.4 mmol). The reaction mixture was stirred overnight and a brown precipitate was removed by filtration. The filtrate was reduced in volume to 10 cm^3 and Et$_2$O (20 cm^3) was added, leading to the formation of a red–brown precipitate which could be recrystallized from MeCN–Et$_2$O. The yield was 0.14 g (47%). The product was spectroscopically identical to that obtained by method A.

2.1.3. (NBu$_4^n$)[Mn$_4$O$_2$(O$_2$CPh)$_7$(imidac)$_2$] (2)

To a stirred solution of Mn(O$_2$CPh)$_2$·2H$_2$O (1.34 g, 4.0 mmol) and PhCO$_2$H (0.86 g, 7.0 mmol) in MeCN (100 cm^3) was slowly added NBu$_4^n$MnO$_4$ (0.36 g, 1.0 mmol) in small portions to give a deep brown solution. To this was added a solution resulting from the combination of imidacH·HCl (0.41 g, 2.5 mmol) in MeCN (5 cm^3) and 1.0 M NBu$_4^n$OH in MeOH (5.0 cm^3, 5.0 mmol). The resulting solution was stirred overnight, filtered through celite, reduced in volume to 40 cm^3, and Et$_2$O (100 cm^3) added dropwise with vigorous stirring. This led to the formation of a red–brown precipitate, which could be recrystallized from MeCN–Et$_2$O. The yield was 1.45 g (73%). Crystals suitable for crystallography were grown by layering an MeCN solution of the complex with Et$_2$O, and they were kept in contact with the mother liquor to prevent interstitial solvent loss. Drying in vacuo leads to the unsolvated form. Elemental analysis. Anal. Found: C, 56.77; H, 5.66; N, 4.34. Calc. for C$_{75}$H$_{81}$N$_5$O$_{20}$Mn$_4$: C, 56.58; H, 5.13; N, 4.40. Selected IR data (cm^{-1}): 1606(s), 1571(s), 1501(w), 1490(m), 1466(w), 1448(m), 1384(s), 1331(s), 1314(m), 1303(m), 1265(m), 1231(w), 1173(m), 1143(w), 1089(w), 1068(w), 1026(m), 940(m), 838(m), 720(s), 690(m), 676(m), 650(s), 630(m), 610(m), 468(m), 437(m).

2.1.4. (NHex$_4^n$)[Mn$_4$O$_2$(O$_2$CMe)$_7$(imidcarb)$_2$] (3)

Method A: to a stirred solution of Mn(O$_2$CMe)$_2$·4H$_2$O (0.74 g, 3.0 mmol) and glacial acetic acid (1 cm^3) in MeCN (70 cm^3) was slowly added NHex$_4^n$MnO$_4$ (0.35 g, 0.75 mmol) in small portions to give a deep brown solution. To this was added a solution resulting from the combination of imidcarbH (0.21 g, 1.9 mmol) in MeCN (10 cm^3) and 0.2 M NHex$_4^n$OH in MeOH (9.5 cm^3, 1.9 mmol). The reaction mixture was stirred overnight and a brown precipitate removed by filtration. The filtrate was reduced in volume to 50 cm^3 and Et$_2$O (100 cm^3) was added, leading to the formation of a red–brown precipitate which could be recrystallized from MeCN–Et$_2$O. The yield was 0.55 g (47%). Drying in vacuo leads to the unsolvated form. Elemental analysis. Anal. Found: C, 44.34; H, 6.28; N, 5.12. Calc. for C$_{46}$H$_{79}$N$_5$O$_{20}$Mn$_4$: C, 44.49; H, 6.41; N, 5.64. Selected IR data (cm^{-1}): 1681(s), 1615(s), 1579(sh), 1504(w), 1486(w), 1465(w), 1397(s), 1332(s), 1313(s), 1263(w),

1188(m), 1154(w), 1099(w), 1076(w), 1043(w), 1013(m), 933(w), 822(m), 800 (w), 776(w), 679(s), 654(s), 614(m), 569(w), 502 (m).

Method B: to a stirred solution of [Mn$_3$O(O$_2$CMe)$_6$-(py)$_3$](ClO$_4$) (0.50 g, 0.57 mmol) in MeCN (60 cm^3) was added a solution resulting from the combination of imidcarbH (0.097 g, 0.86 mmol) in MeCN (5 cm^3) and 0.2 M NHex$_4^n$OH in MeOH (4.3 cm^3, 0.86 mmol). The reaction mixture was stirred overnight and a brown precipitate was removed by filtration. The filtrate was reduced in volume to 30 cm^3 and Et$_2$O (60 cm^3) was added, leading to the formation of a red–brown precipitate which could be recrystallized from MeCN–Et$_2$O. The yield was 0.27 g (50%). The product was spectroscopically identical to that obtained by method A.

2.1.5. (NHex$_4^n$)[Mn$_4$O$_2$(O$_2$CPh)$_7$(imidcarb)$_2$] (4)

To a stirred solution of Mn(O$_2$CPh)$_2$·2H$_2$O (0.49 g, 1.5 mmol) and PhCO$_2$H (0.32 g, 2.6 mmol) in MeCN (80 cm^3) was slowly added NHex$_4^n$MnO$_4$ (0.17 g, 0.36 mmol) in small portions to give a deep brown solution. To this was added a solution resulting from the combination of imidcarbH (0.10 g, 0.92 mmol) in MeCN (5 cm^3) and 0.2 M NHex$_4^n$OH in MeOH (4.6 cm^3, 0.92 mmol). The resulting solution was stirred overnight, filtered through celite, reduced in volume to 40 cm^3, and Et$_2$O (100 cm^3) added dropwise with vigorous stirring. This led to the formation of a red–brown

Table 1
Crystallographic data for complex **2**·5MeCN

Formula [a]	C$_{85}$H$_{96}$Mn$_4$N$_{10}$O$_{20}$
Formula weight	1797.50
Space group	P$\bar{1}$
Crystal system	triclinic
a (Å)	12.1886(3)
b (Å)	17.8130(5)
c (Å)	22.0268(5)
α (°)	68.1714(8)
β (°)	84.7029(8)
γ (°)	83.0696(7)
V (Å^3)	4401.2
Z	2
Temperature (°C)	−163
Crystal size (mm)	0.60 × 0.40 × 0.40
Radiation (Å) [b]	0.71073
ρ (g cm^{-3})	1.356
μ (cm^{-1})	6.344
Collected data (°)	4.92 ≤ 2θ ≤ 54.57
Total data	35889
Unique data	20163
R_{merge}	0.038
Observed data ($F > 2\sigma(F)$)	10514
R (%) [c]	6.07
R_w (%) [d]	6.19

[a] Including solvate molecules.
[b] Graphite monochromator.
[c] $R = 100 \ \Sigma||F_o| - |F_c||/\Sigma|F_o|$.
[d] $R_w = 100 \ [\Sigma w(|F_o| - |F_c|)^2/\Sigma w|F_o|^2]^{1/2}$ where $w = 1/\sigma^2(|F_o|)$.

precipitate, which could be recrystallized from MeCN–Et$_2$O. The yield was 0.12 g (54%). Drying in vacuo leads to the unsolvated form. Elemental analysis. *Anal.* Found: C, 57.50; H, 5.57; N, 4.18. Calc. for C$_{81}$H$_{93}$N$_5$O$_{20}$Mn$_4$: C, 58.03; H, 5.59; N, 4.18. Selected IR data (cm^{-1}): 1680(s), 1610(s), 1572(s), 1508(w), 1490(w), 1464(w), 1448(m), 1375(s), 1344(sh), 1305(s), 1188(w), 1174(m), 1156(w), 1140(w), 1068(m), 1025(m), 1012(m), 936(w), 827(m), 780(w), 718(s), 688(m), 676(m), 654(s), 617(m), 563(w), 502(m), 468(m).

2.2. X-ray crystallography

Data for complex **2** were collected on a Bruker platform goniometer equipped with a SMART 6000 CCD detector at −163°C; details of the diffractometry, low temperature facilities and computational procedures employed by the Molecular Structure Center are available elsewhere [11]. Data collection parameters are summarized in Table 1.

The initial survey of a limited portion of reciprocal space located a set of reflections with no symmetry or systematic absences. Solution and refinement of the structure confirmed the choice of the centrosymmetric space group P$\bar{1}$. The structure was solved using a combination of Patterson and direct methods (DIRDIF-96 [12]). Most of the atoms in the cation and anion were located from DIRDIF-96. The remaining atoms were located in successive iterations of least-squares refinement followed by generation of a difference Fourier map. In addition to the main anion of interest, the asymmetric unit contained a NBu$_4^{n+}$ cation and five molecules of MeCN. Many of the hydrogen atoms were visible in a later difference Fourier map. On three of the solvent molecules, at least one hydrogen atom was located on the methyl carbon atom. Hydrogen atoms were then introduced in fixed calculated positions and assigned a thermal parameter of 1.0 plus the isotropic equivalent of the parent atom. In the final cycles of least-squares refinement the non-hydrogen atoms were refined using anisotropic thermal parameters, while the hydrogen atoms were fixed. The final difference map was essentially featureless, the largest peak was 1.42 e Å^{-3} located 1.05 Å from H(55) and 1.92 Å from C(93) (in the cation). The next largest peak was 0.98 e Å^{-3} also in the region of the cation, indicating a possible small disorder.

2.3. Other measurements

IR spectra (KBr pellet) were recorded on a Nicolet model 510P spectrometer. ^{1}H NMR spectra were recorded in CD$_3$CN at ~20°C with a 300 MHz Varian Gemini 2000 NMR spectrometer. Cyclic voltammetry employed a BAS CV-50W voltammetric analyzer and a standard three-electrode assembly (glassy-carbon work-

Fig. 1. ORTEP representation for the anion of complex **2** at the 50% probability level. For clarity, only the *ipso* carbon atom of each benzoate ring is included.

ing, Pt-wire auxiliary, Ag–AgNO$_3$ reference) with 0.1 M NBu$_4^n$PF$_6$ as supporting electrolyte. Potentials are quoted versus the ferrocene–ferrocenium couple under the same conditions. Elemental Analyses were performed by Atlantic Microlab Inc., Norcross, Georgia or in-house with a Perkin–Elmer Series II CHNS/O Analyzer 2000.

3. Results and discussion

3.1. Syntheses

In earlier reports we have described two procedures for the preparation of $[Mn_4^{III}O_2(O_2CR)_7(L)_2]^z$ complexes, where L is derived from 2,2′-bipyridine (bpy), picolinic acid (picH), 8-hydroxyquinoline (hqnH) and 2-(hydroxymethyl)pyridine (hmpH) [4–6] The first procedure involves treatment of trinuclear $[Mn_3O(O_2CR)_6$-$(py)_3]^+$ complexes with salts of the chelating ligand L, or with the acid form of the ligand and an equivalent of base. The second procedure involves a comproportion-ation reaction between Mn^{II} and MnO$_4^-$ in the presence of RCO$_2$H and L. In the present study both procedures have allowed the synthesis of the analogous imidac$^-$ and imidcarb$^-$ complexes with R = Me and Ph. NBu$^{n+}_4$ salts of the imidac$^-$ species were isolated, while NHex$_4^{n+}$ salts of the imidcarb$^-$ species were preferred in order to obtain soluble materials. Thus, treatment of an MeCN solution of $[Mn_3O(O_2CMe)_6(py)_3]^+$ with NBu$_4^n$(imidac) or NHex$_4^n$(imidcarb) generated in situ afforded a brown solution from which NBu$_4^n$[Mn$_4$O$_2$-$(O_2CMe)_7(imidac)_2]$ (**1**) or NHex$_4^n$[Mn$_4$O$_2$(O$_2$CMe)$_7$-$(imidcarb)_2]$ (**3**) were obtained with minimal workup in good yield (47 and 50%, respectively). Employment of the second procedure, whereby a reaction mixture containing Mn(O$_2$CR)$_2$, NR$_4'$MnO$_4$ (R′ = Bu^n or Hex^n) and RCO$_2$H was similarly treated with NBu$_4^n$(imidac) or NHex$_4^n$(imidcarb) also resulted in brown solutions from

which **1**, NBu$_4^n$[Mn$_4$O$_2$(O$_2$CPh)$_7$(imidac)$_2$] (**2**), **3** and NHex$_4^n$[Mn$_4$O$_2$(O$_2$CPh)$_7$(imidcarb)$_2$] (**4**) were obtained with minimal workup in good yield (55, 73, 47 and 54%, respectively). This reaction employed a 4:1 Mn$_4^{II}$:Mn^{VII} ratio, as required for preparation of a Mn$_4^{III}$ product (Eq. (1))

$$4Mn^{2+} + Mn^{7+} \rightarrow 5/4Mn_4^{3+} \tag{1}$$
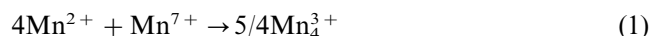
Compound **2** was structurally characterized, and all available characterization data for **1** are consistent with it having the same structure as **2**. Crystals of **3** and **4** suitable for X-ray crystallography could not be obtained; however, all of the characterization data are consistent with structures analogous to those of **1** and **2**.

3.2. Description of structure

An ORTEP representation of the anion of complex **2** is given in Fig. 1. Crystallographic data and selected bond distances and angles are listed in Tables 1 and 2, respectively.

Complex **2** crystallizes in the triclinic space group $P\bar{1}$. The asymmetric unit contains the complete anion, the NBu$_4^{n+}$ cation and five MeCN solvate molecules; the latter two will not be further discussed. The anion of **2** possesses a Mn$_4$O$_2$ core with the familiar 'butterfly' structure. Mn(1) and Mn(2) occupy the 'body' positions, while Mn(3) and Mn(4) occupy the 'wingtip' positions and O(5) and O(6) triply bridge each wing. The structure can be considered as two triangular Mn$_3$O units edge-shared through Mn(1) and Mn(2) with a dihedral angle of 142.2°. Unlike the planar core of the Mn$_3$O complexes, the μ_3-O atoms of the triangular units of the 'butterfly' structure lie slightly below the plane (Fig. 1). Two distinct Mn···Mn distances are observed, with the 'body' Mn(1)···Mn(2) separation of ca. 2.8 Å significantly shorter than the four 'body' to 'wingtip' separations of 3.3–3.4 Å. These separations are consistent with the presence of two and one bridg-ing oxygen atoms, respectively [13]. Peripheral ligation is by seven bridging benzoate ligands and two imidac$^-$ ligands chelating the 'wingtip' Mn atoms. Each Mn atom is six-coordinate with axially elongated octahedral geometry typical of Jahn–Teller distorted high spin d^4 Mn^{III} ions. The axially elongated sites are all occupied by benzoate oxygen atoms, with both of the oxygen atoms of the unique benzoate ligand (bridging the 'body' Mn atoms) occupying JT elongated positions. The imidac$^-$ oxygen atoms are coordinated *trans* to the μ_3-O atoms at a distance of 1.9 Å, which is comparable to the other (non-JT elongated) Mn-benzoate bonds. The molecule has idealized C_2 point symmetry and, overall, the structure is extremely similar to those of the analogous bpy, pic$^-$, hqn$^-$ and hmp$^-$ complexes, with the cores of each species essentially superimposable

[4–6]. The structural differences between complex **2** and the previously reported 'butterfly' complexes arise in the vicinity of the chelating ligand. In particular, the imidac$^-$ species possesses a significantly non-planar six-membered chelate ring in contrast to the planar five-membered chelate rings of the bpy, pic$^-$, hqn$^-$ and hmp$^-$ species.

Table 2
Selected interatomic distances (Å) and angles (°) for complex **2**

Mn(1)···Mn(2)	2.816(1)	Mn(2)···Mn(3)	3.293(1)
Mn(1)···Mn(3)	3.446(1)	Mn(2)···Mn(4)	3.444(1)
Mn(1)···Mn(4)	3.319(1)		
Mn(1)–O(5)	1.915(3)	Mn(3)–O(5)	1.848(3)
Mn(1)–O(6)	1.872(3)	Mn(3)–O(18)	2.244(4)
Mn(1)–O(7)	2.156(3)	Mn(3)–O(36)	2.201(4)
Mn(1)–O(16)	1.958(3)	Mn(3)–O(63)	1.933(3)
Mn(1)–O(25)	1.981(3)	Mn(3)–O(77)	1.929(4)
Mn(1)–O(52)	2.175(3)	Mn(3)–N(70)	2.012(4)
Mn(2)–O(5)	1.869(3)	Mn(4)–O(6)	1.876(3)
Mn(2)–O(6)	1.898(3)	Mn(4)–O(27)	2.166(3)
Mn(2)–O(9)	2.240(3)	Mn(4)–O(45)	2.176(3)
Mn(2)–O(34)	1.971(4)	Mn(4)–O(54)	1.957(3)
Mn(2)–O(43)	1.942(3)	Mn(4)–O(86)	1.903(3)
Mn(2)–O(61)	2.205(3)	Mn(4)–N(79)	2.027(4)
Mn(1)–O(5)–Mn(2)	96.2(2)	Mn(1)–O(6)–Mn(4)	124.7(2)
Mn(1)–O(6)–Mn(2)	96.7(2)	Mn(2)–O(5)–Mn(3)	124.8(2)
Mn(1)–O(5)–Mn(3)	132.6(2)	Mn(2)–O(6)–Mn(4)	131.7(2)
O(5)–Mn(1)–O(6)	82.7(2)	O(5)–Mn(3)–O(18)	92.3(2)
O(5)–Mn(1)–O(7)	86.0(2)	O(5)–Mn(3)–O(36)	96.0(2)
O(5)–Mn(1)–O(16)	91.7(2)	O(5)–Mn(3)–O(63)	94.2(2)
O(5)–Mn(1)–O(25)	172.6(2)	O(5)–Mn(3)–O(77)	176.6(2)
O(5)–Mn(1)–O(52)	98.8(2)	O(5)–Mn(3)–N(70)	90.9(2)
O(6)–Mn(1)–O(7)	92.8(2)	O(18)–Mn(3)–O(36)	171.5(2)
O(6)–Mn(1)–O(16)	172.4(2)	O(18)–Mn(3)–O(63)	87.3(2)
O(6)–Mn(1)–O(25)	99.7(2)	O(18)–Mn(3)–O(77)	84.8(2)
O(6)–Mn(1)–O(52)	89.6(2)	O(18)–Mn(3)–N(70)	93.1(2)
O(7)–Mn(1)–O(16)	92.0(2)	O(36)–Mn(3)–O(63)	90.3(2)
O(7)–Mn(1)–O(25)	86.8(2)	O(36)–Mn(3)–O(77)	87.0(2)
O(7)–Mn(1)–O(52)	174.8(2)	O(36)–Mn(3)–N(70)	88.6(2)
O(16)–Mn(1)–O(25)	86.5(2)	O(63)–Mn(3)–O(77)	87.5(2)
O(16)–Mn(1)–O(52)	86.1(2)	O(63)–Mn(3)–N(70)	175.0(2)
O(25)–Mn(1)–O(52)	88.3(2)	O(77)–Mn(3)–N(70)	87.5(2)
O(5)–Mn(2)–O(6)	83.2(2)	O(6)–Mn(4)–O(27)	92.5(2)
O(5)–Mn(2)–O(9)	89.8(2)	O(6)–Mn(4)–O(45)	89.7(2)
O(5)–Mn(2)–O(34)	98.4(2)	O(6)–Mn(4)–O(54)	94.9(2)
O(5)–Mn(2)–O(43)	174.4(2)	O(6)–Mn(4)–O(86)	176.1(2)
O(5)–Mn(2)–O(61)	86.8(2)	O(6)–Mn(4)–N(79)	90.2(2)
O(6)–Mn(2)–O(9)	85.0(2)	O(27)–Mn(4)–O(45)	174.1(2)
O(6)–Mn(2)–O(34)	171.8(2)	O(27)–Mn(4)–O(54)	91.6(2)
O(6)–Mn(2)–O(43)	94.8(2)	O(27)–Mn(4)–O(86)	91.1(2)
O(6)–Mn(2)–O(61)	98.6(2)	O(27)–Mn(4)–N(79)	86.1(2)
O(9)–Mn(2)–O(34)	87.0(2)	O(45)–Mn(4)–O(54)	93.7(2)
O(9)–Mn(2)–O(43)	95.3(2)	O(45)–Mn(4)–O(86)	86.6(2)
O(9)–Mn(2)–O(61)	174.7(2)	O(45)–Mn(4)–N(79)	88.4(2)
O(34)–Mn(2)–O(43)	84.4(2)	O(54)–Mn(4)–O(86)	86.7(2)
O(34)–Mn(2)–O(61)	89.5(2)	O(54)–Mn(4)–N(79)	174.5(2)
O(43)–Mn(2)–O(61)	88.3(2)	O(86)–Mn(4)–N(79)	88.4(2)

3.3. ^1H NMR spectroscopy

The ^1H NMR spectra of complexes **1** and **2** in MeCN-d_3 are shown in Fig. 2 and the resonance positions are listed in Table 3 using the labeling scheme given in Fig. 2. Assignments were made on the basis of: (i) comparison with the spectrum of the O$_2$CMe-d_3 analog of **1** to distinguish between the resonances of the imidac$^-$ protons and those associated with the carboxylates; (ii) addition of D$_2$O to the NMR solution to assign the amine resonance of the imidac$^-$ ligand; (iii) T_1 measurements (inversion recovery method) correlated with the relative proton to metal centre distances to assign the remaining resonances associated with the imidac$^-$ protons; and (iv) comparison with the spectra of structurally analogous 'butterfly' complexes with other chelating ligands [5,6]. Both complexes display five resonances due to the protons of the imidac$^-$ ligand in addition to resonances due to the carboxylate protons.

For complex **1** four resonances due to the methyl protons of the four inequivalent acetate ligands are observed with an approximate intensity ratio of 2:2:2:1, indicating that the peak at 16.9 ppm (C′) can be assigned to the unique acetate bridging the 'body' Mn atoms Mn(1) and Mn(2). The resonance positions and T_1 values of these four resonances are similar to those observed for the pic$^-$ and hqn$^-$ 'butterfly' complexes and are consistent with idealized C_2 point symmetry, implying retention of the solid state structure in solution. A more complex spectrum is evident for **2** due to the presence of four inequivalent benzoate ligands. Assignment of the resonances as due to *ortho*, *meta* or *para* protons may be broadly made on the basis of the relative chemical shifts and T_1 values [14], although it is not possible to ascertain which peaks correspond to the unique benzoate ligand bridging the 'body' Mn atoms. Nevertheless, the pattern of benzoate resonances is again similar to that observed for other benzoate 'butterfly' complexes.

Five resonances of approximately equal intensity are observed for the protons of the imidac$^-$ ligands for both complexes **1** and **2**. For complex **1** the most downfield imidac$^-$ resonance at ca. 26.3 ppm is obscured by a resonance due to the protons of the unique acetate ligand and is only evident in the spectrum of the O$_2$CMe-d_3 analogue. Addition of a small amount of D$_2$O to the NMR solutions of **1** and **2** leads to the immediate disappearance of the resonances at −2.5 and −4.3 ppm, respectively. This is attributed to exchange broadening and allows assignment of these resonances to the amine proton of the imidac$^-$ ligand, H$_B$. Assignment of the remaining resonances relies predominantly on the correlation between the line widths, measured T_1 values and the proton to 'wingtip' metal centre [Mn(3) and Mn(4)] separations derived from the crystal
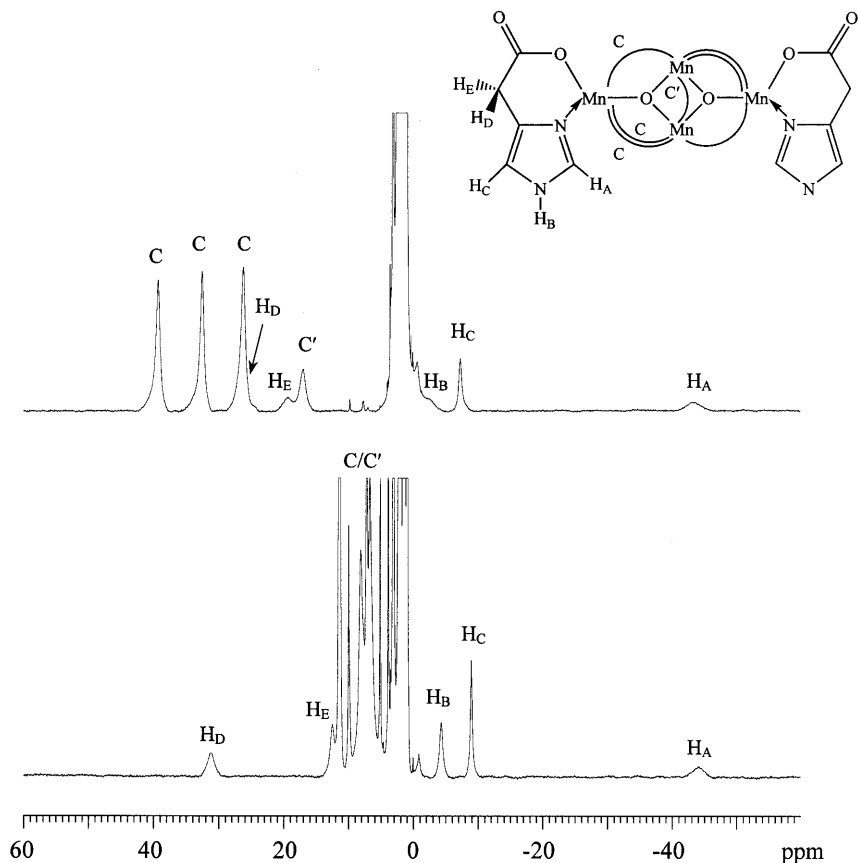
Fig. 2. Proton NMR spectra of complexes **1** (top) and **2** (bottom) in MeCN-d_3. The peaks are labeled according to the scheme shown as an inset. The band of resonances in the -1 to 5 ppm region is from the NBu_4^{n+} protons, residual protio solvent and adventitious water.

Table 3
Proton NMR data for complexes **1** and **2** in MeCN-d_3 at $T \sim 20°C$

Complex **1**		Complex **2**		Assignment [a]
δ (ppm)	T_1 (ms) [b]	δ (ppm)	T_1 (ms) [b]	
39.2	2.2			C (A)
32.4	2.4			C (A)
26.3 [c]	0.9 [c]	31.2	0.8	H_D
26.1	2.0			C (A)
19.3	1.3	12.5	2.2	H_E
16.9	2.2			C (A') [d]
		11.5	17.3	C (m-B)
		11.3	16.1	C (m-B)
		10.0	12.2	C (m-B)
		8.1	2.5	C (o-B)
		7.2	9.2	C (o-B)
		6.6	5.2	C (o-B)
		5.1	32.1	C (p-B)
		3.9	31.2	C (p-B)
-2.5	[e]	-4.3	4.0	H_B
-7.3	3.3	-8.9	4.9	H_C
-42.9	0.5	-44.2	0.5	H_A

[a] Numbering of imidac$^-$ protons as in Fig. 2.
[b] Inversion recovery method.
[c] Determined from (O_2CMe-d_3) analog of **1**.
[d] Unique acetate bridging Mn(1) and Mn(2).
[e] Could not be determined.
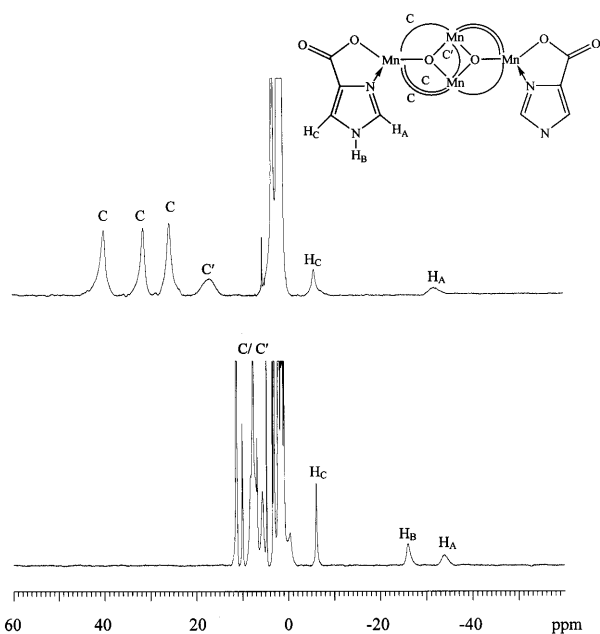
Fig. 3. Proton NMR spectra of complexes **3** (top) and **4** (bottom) in MeCN-d_3. The peaks are labeled according to the scheme shown as an inset. The band of resonances in the -1 to 5 ppm region is from the $NHex_4^{n+1}$ protons, residual protio solvent and adventitious water.

Table 4
Proton NMR data for complexes **3** and **4** in MeCN-d_3 at $T \sim 20°C$

Complex **3**		Complex **4**		Assignment [a]
δ (ppm)	T_1 (ms) [b]	δ (ppm)	T_1 (ms) [b]	
39.9	2.4			C (A)
31.3	2.4			C (A)
25.6	2.3			C (A)
16.8	2.4			C (A′) [c]
		11.3	19.0	C (m-B)
		11.2	18.1	C (m-B)
		10.0	13.8	C (m-B)
		8.2	d	C (o-B)
		7.6	8.9	C (o-B)
		6.8	12.8	C (o-B)
		5.7	2.4	C (o-B)
		4.7	36.2	C (p-B)
		3.4	32.5	C (p-B)
−5.8	2.6	−6.1	4.5	H_C
d	d	−25.8	d	H_B
−32.0	0.3	−33.9	0.6	H_A

[a] Numbering of imidcarb$^-$ protons as in Fig. 3.
[b] Inversion recovery method.
[c] Unique acetate bridging Mn(1) and Mn(2).
[d] Could not be determined.
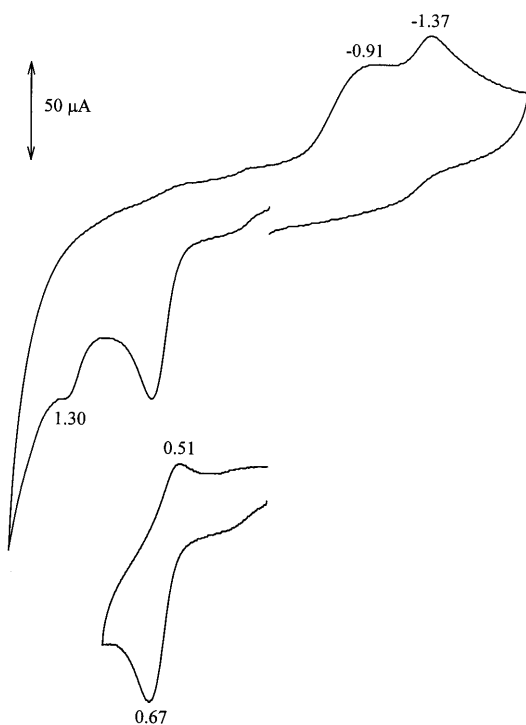
Fig. 4. Cyclic voltammogram (1 mM, 100 mV s^{-1}) for complex **2** in MeCN (0.1 M NBu$_4^n$PF$_6$). The potentials (V) are quoted versus ferrocene–ferrocenium.

structure of **2**. This is on the basis of previous studies that have concluded that the major contibution to the line widths in Mn^{III} complexes is dipolar broadening, which is proportional to r^{-6} [15–18]. The broadest resonance, with the smallest T_1 value, at ca. −40 ppm

is assigned to the proton closest to the wingtip Mn atoms, H_A. The significant upfield chemical shift of this resonance is consistent with those observed for the proton at the position adjacent to the Mn-coordinated N atoms in the pic$^-$ and hqn$^-$ 'butterfly' compounds. The sharpest resonance with the largest T_1 value is assigned to the proton most distant from the Mn centre, H_C. Protons H_D and H_E are diastereotopic with H_D significantly closer to the Mn atom (ca. 3.5 versus 4.2 Å), and are assigned accordingly. The marked chemical shift difference between the resonances of these protons indicates the significant contribution of a dipolar mechanism to the observed isotropic shifts. The chemical shifts of resonances H_A, H_B and H_C are relatively consistent between complexes **1** and **2**, with less than 2 ppm difference observed in each case. However, slightly larger chemical shift differences of ca. 5 and 7 ppm are observed for H_D and H_E, respectively. The reason for this is unclear in the absence of a crystal structure of complex **1**.

The ^{1}H NMR spectra of complexes **3** and **4** in MeCN-d_3 are shown in Fig. 3 and the resonance positions are listed in Table 4 using the labeling scheme given in Fig. 3. Assignments were made analogously to those for **1** and **2**. The pattern of resonances due to the carboxylate protons of **3** and **4** are very similar to those observed for **1** and **2**. Three resonances due to the imidcarb$^-$ protons are observed for **4** while only two are evident for **3**. The one missing is that due to H_B, which is presumably because of exchange with adventitious water. The resonances due to H_A and H_C display very similar isotropic shifts to the equivalent resonances in **1** and **2**, while the resonance due to H_B is shifted by ca. 20 ppm, presumably due to exchange effects.

3.4. Electrochemistry

The cyclic voltammograms (CVs) of complexes **1** and **2** (1 mM) have been recorded in MeCN solution (0.1 M NBu$_4^n$PF$_6$) (Fig. 4). Similar results are observed for both complexes and the CV of **2** is shown in Fig. 3. Both complexes display a quasi-reversible one-electron oxidation at 0.58 and 0.59 V versus ferrocene for **1** and **2**, respectively. The peak separations at a scan rate of 100 mV s^{-1} are 187 and 154 mV, respectively, compared with that for the ferrocene–ferrocenium couple of 116 mV under the same conditions. Plots of i_p versus $v^{1/2}$ are linear in the scan rate (v) range of 10–500 mV s^{-1}, indicating a diffusion-controlled process. Both complexes also display an irreversible oxidation at peak potentials of 1.35 and 1.30 V, respectively at a scan rate of 100 mV s^{-1}. In addition two irreversible reductions are observed at peak potentials of −0.94 and −1.37 for **1** and −0.91 and −1.37 V for **2**.

The quasi-reversible oxidation at 0.59 V for **2** in MeCN is assigned to oxidation to the Mn$_3^{III}$Mn^{IV} level

as shown in Eq. (2). The oxidation potential can be compared with the

$$[Mn_4O_2(O_2CPh)_7(imidac)_2]^- \overset{0.59\ V}{\rightleftharpoons}$$

$$[Mn_4O_2(O_2CPh)_7(imidac)_2]^0 \tag{2}$$
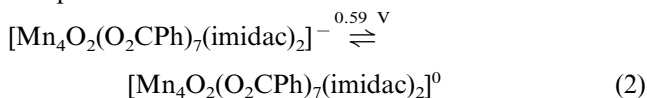
value of 0.69 V found for the corresponding couple in $[Mn_4O_2(O_2CPh)_7(pic)_2]^-$ under the same conditions. This is consistent with the greater acidity of picH (pK_a of 5.25 [19]) versus imidacH (pK_a measured as ca. 7.0), as the more electron-donating imidac$^-$ is better able to stabilize higher oxidation states of Mn than pic$^-$.

Well-defined cyclic voltammograms of complexes **3** and **4** could not be obtained due to their relative insolubility in MeCN in the presence of 0.1 M $NBu_4^nPF_6$ as support electrolyte. However, poorly resolved oxidation processes with peak potentials of ca. 0.60 and 1.2 V and reduction processes at ca. -1.2 and -1.6 V were evident for **4** under these conditions.

The presence of apparently accessible oxidation processes for complexes **1** and **2** suggested the possibility of oxidation of these complexes. Indeed, oxidation of other 'butterfly' complexes has resulted in the formation of new species [20]. An investigation of similar reactivity for **1** and **2** is in progress, with preliminary studies involving electrochemical oxidation of these species resulting in insoluble red–brown solids. Further efforts are required to fully characterize these materials, although their IR spectra do not display bands associated with NBu_4^{n+}, implying that they are uncharged.

4. Conclusions

Tetranuclear Mn clusters possessing imidazole-carboxylate based chelating ligands have been synthesized and found to be essentially isostructural with those possessing pyridine-based chelating ligands. ^1H NMR spectroscopy indicates that the species retain their structure in solution and the resonances can be assigned using the methods described in the text. An investigation of the electrochemistry of the species reveals a quasi-reversible oxidation process, similar to those observed for the analogous compounds possessing pyridine-based chelating ligands.

5. Supplementary data

Supplementary structural data for compound **2** have been deposited with the Cambridge Crystallographic Data Centre, CCDC No. 141954. Copies of this information may be obtained free of charge from The Director, CCDC, 12 Union Road, Cambridge, CB2 1EZ, UK (fax: + 44-1223-336033; e-mail: deposit@ccdc.ac.uk or www: http://www.ccdc.cam.ac.uk).

References

[1] G. Aromi, S.M.J. Aubin, M.A. Bolcar, G. Christou, H.J. Eppley, K. Folting, D.N. Hendrickson, J.C. Huffman, R.C. Squire, H.L. Tsai, S. Wang, M.W. Wemple, Polyhedron 17 (1998) 3005 and references cited therein.
[2] V.K. Yachandra, K. Sauer, M.P. Klein, Chem. Rev. 96 (1996) 2927.
[3] J.R. Debus, Biochim. Biophys. Acta 1102 (1992) 269.
[4] J.B. Vincent, C. Christmas, H.R. Chang, Q. Li, P.D.W. Boyd, J.C. Huffman, D.N. Hendrickson, G. Christou, J. Am. Chem. Soc. 111 (1989) 2086.
[5] E. Libby, J.K. McCusker, E.A. Schmitt, K. Folting, D.N. Hendrickson, G. Christou, Inorg. Chem. 30 (1991) 3486.
[6] E. Bouwman, M.A. Bolcar, E. Libby, J.C. Huffman, K. Folting, G. Christou, Inorg. Chem. 31 (1992) 5185.
[7] X.-S. Tang, B.A. Diner, B.S. Larsen, M.L. Gilchrist, G.A. Lorigan, R.D. Britt, Proc. Nat. Acad. Sci. USA 91 (1994) 704.
[8] J.B. Vincent, H.R. Chang, K. Folting, J.C. Huffman, G. Christou, D.N. Hendrickson, J. Am. Chem. Soc. 109 (1987) 5703.
[9] J.B. Vincent, K. Folting, J.C. Huffman, G. Christou, Inorg. Chem. 25 (1986) 996.
[10] T.J. Giovanellio, J. Pecci, Clin. Chim. Acta 67 (1976) 7.
[11] M.H. Chisholm, K. Folting, J.C. Huffman, C.C. Kirkpatrick, Inorg. Chem. 23 (1984) 1021.
[12] P.T. Beurskins, G. Beurskins, W.P. Bosman, R. de Gelder, S. Garcia Granda, R.O. Gould, R. Israel, J.M.M. Smits, DIRDIF-96, A Computer Program System for Crystal Structure Determination by Patterson Methods and Direct Methods applied to Difference Structure Factors, University of Nijmegen, The Netherlands (1996).
[13] G. Christou, J.B. Vincent, in: L. Que (Ed.), ACS Symposium Series 372, American Chemical Society, Washington DC, 1988, p. 238 (Chapter 12).
[14] M.M. Glass, K. Belmore, J.B. Vincent, Polyhedron 12 (1993) 133.
[15] P. Addy, D.F. Evans, Q. De Souza, Polyhedron 6 (1987) 2003.
[16] D.R. Eaton, J. Am. Chem. Soc. 87 (1965) 3097.
[17] G.N. La Mar, F.A. Walker, J. Am. Chem. Soc. 95 (1973) 6950.
[18] G.N. La Mar, W.DeW. Horrocks, R.H. Holm (Eds.), NMR of Paramagnetic Molecules, Academic Press, New York, 1973.
[19] E.P. Sergeant, B. Dempsey, Ionisation Constants of Organic Acids in Aqueous Solution, Pergamon, Oxford, 1979.
[20] S. Wang, H.L. Tsai, K.S. Hagen, D.N. Hendrickson, G. Christou, J. Am. Chem. Soc. 116 (1994) 8376.